Supplementary Materials

Macromolecular Crowding as a Regulator of Gene Transcription

H. Matsuda, G.G. Putzel, V. Backman, and I. Szleifer

1 Numerical estimates of model parameters

Here we determine numerical estimates of the parameters appearing in the model, namely, the reaction rates and the total concentrations of the reagents. The rates are determined from the microscopic theory of facilitated diffusion developed by Berg and coworkers (1–3). Our estimates are made assuming dilute conditions (nuclear crowder volume fraction $\phi = 0$). We do not concern ourselves with the rates of the irreversible reactions following pre-mRNA production, such as splicing and mRNA export, since they do not influence the steady-state results.

Assuming that non-specific binding of TF and RNAp to DNA is diffusion-limited, we use the following expression (1–3) for the forward rates k_1 and k_3:

$$k_{\mathrm{t}}^{\mathrm{ns}} = \frac{2\pi D_{\mathrm{TF}} l}{\ln(\xi/2b)} \qquad k_{\mathrm{f}}^{\mathrm{ns}} = \frac{2\pi D_{\mathrm{RNAp}} l}{\ln(\xi/2b)} \tag{1}$$

Here D_{TF} and D_{RNAp} are the diffusion coefficients of TF and RNAp, given by the Stokes-Einstein formula

$$D_{\mathrm{TF}} = \frac{k_B T}{6\pi\eta r_{\mathrm{TF}}} \qquad D_{\mathrm{RNAp}} = \frac{k_B T}{6\pi\eta r_{\mathrm{RNAp}}}$$

We assume a temperature of $37^\circ\,\mathrm{C} = 310\,\mathrm{K}$, at which the dynamic viscosity of water is $\eta = 6.5 \times 10^{-4}\,\mathrm{J \cdot s/m^3}$. We are modeling the RNA polymerase as a sphere of radius $r_{\mathrm{RNAp}} = 5.4\,\mathrm{nm}$ and the TF as a sphere of radius $r_{\mathrm{TF}} = 4\,\mathrm{nm}$, giving $D_{\mathrm{TF}} = 8.7 \times 10^{-11}\,\mathrm{m^2/s}$ and $D_{\mathrm{RNAp}} = 6.4 \times 10^{-11}\,\mathrm{m^2/s}$.

The definitions of the variables ξ, b, and l are as follows. ξ is the correlation length for the DNA, that is, the typical distance between neighboring DNA segments. This correlation length will vary depending on the physical arrangement of the DNA into loops, chromatin territories, etc. We choose $\xi = 20\,\mathrm{nm}$, keeping in mind that these rates will vary weakly with ξ; we have

checked that varying ξ in either direction by a factor of 4 does not affect our qualitative results. Two more lengths appear in Eq. 1: the radius b of the DNA molecule, about 1 nm, and the length l along the DNA of one base pair, namely 0.34 nm. Using these values, we have non-specific association rate constants in the absence of crowding:

$$k_{\mathrm{t}}^{\mathrm{ns}} = 4.9 \times 10^4\,\mathrm{mM}^{-1}\mathrm{s}^{-1} \qquad k_{\mathrm{f}}^{\mathrm{ns}} = 3.6 \times 10^4\,\mathrm{mM}^{-1}\mathrm{s}^{-1}$$

The nonspecific dissociation rates follow from the dissociation constants for non-specific binding, called $K_{D,\mathrm{TF}}^{\mathrm{n.s.}}$ and $K_{D,\mathrm{RNAp}}^{\mathrm{n.s.}}$. We take these to be both equal to 1 mM in the absence of crowding, giving

$$k_{\mathrm{o}}^{\mathrm{ns}} = K_{D,\mathrm{TF}}^{\mathrm{n.s.}} \cdot k_{\mathrm{t}}^{\mathrm{ns}} = 4.9 \times 10^4\,\mathrm{s}^{-1} \qquad k_{\mathrm{b}}^{\mathrm{ns}} = K_{D,\mathrm{RNAp}}^{\mathrm{n.s.}} \cdot k_{\mathrm{f}}^{\mathrm{ns}} = 3.6 \times 10^4\,\mathrm{s}^{-1}$$

The association rate constants for specific binding of TF and RNAp are given by the expression derived by Berg et al. (2) for specific protein-DNA binding by facilitated diffusion:

$$k_{\mathrm{t}} = V \cdot (D_{1,\mathrm{TF}} \cdot k_{\mathrm{o}}^{\mathrm{ns}})^{1/2}/L \qquad k_{\mathrm{f}} = V \cdot (D_{1,\mathrm{RNAp}} \cdot k_{\mathrm{b}}^{\mathrm{ns}})^{1/2}/L \tag{2}$$

The factor of V representing the volume of the nucleus does not appear in the expression of Berg et al. (2). This is due to the fact that in the reaction equations Eqs. 4 and 5 we take the forward rates to multiply the product of the *volume* densities (concentrations) of both reagents, in such a way that the association rate constants have the usual dimensions of concentration$^{-1}\times$time^{-1}. We use a typical volume for a HeLa cell of $V = 500\,\mu\mathrm{m}^3$ (4, 5). The length L is one-half of the total length of genomic DNA. A diploid human cell (before S phase) contains 6×10^9 bp. This corresponds to $L = 1\,\mathrm{m}$. The quantities $D_{1,\mathrm{TF}}$ and $D_{1,\mathrm{RNAp}}$ are the one-dimensional diffusion coefficients for motion of TF and RNAp along DNA. Elf et al. (6) report a value of $D_1 = 0.046\,\mu\mathrm{m}^2/s$ for a transcription factor, which is about 100 times smaller than the TF's three-dimensional diffusion coefficient. Assuming that the protein follows a helical path winding around the DNA as has been found experimentally (7), Bagchi et al. (8) derived a formula for the one-dimensional diffusion coefficient of a protein non-specifically bound to DNA:

$$D_1 = \frac{k_B T}{\zeta_{\mathrm{trans}}^{\mathrm{total}}},$$

where

$$\zeta_{\mathrm{trans}}^{\mathrm{total}} = 6\pi\eta R + \left(\frac{2\pi}{10l}\right)^2 \left[8\pi\eta R^3 + 6\pi\eta R (R_{\mathrm{OC}})^2\right]$$

Here R is the radius of the spherical protein while $R_{\rm OC}$ is the distance between the centers of mass of the protein and DNA. The integer 10 appears because this is the number of base pairs (of length $l = 0.34\,\mathrm{nm}$) per turn of DNA. Using the radii of the TF and RNAp we find

$$D_{1,\mathrm{TF}} = \frac{D_{3,\mathrm{TF}}}{157.3} \qquad D_{1,\mathrm{RNAp}} = \frac{D_{3,\mathrm{RNAp}}}{270.4}$$

Using these numerical values, we obtain

$$k_{\rm t} = 0.05\,\mathrm{nM}^{-1}\mathrm{s}^{-1} \qquad k_{\rm f} = 0.03\,\mathrm{nM}^{-1}\mathrm{s}^{-1} \tag{3}$$

The backward rates for specific binding are determined from (2)

$$\frac{k_{\rm o}}{k_{\rm t}} = [D]_{\rm tot} \cdot \frac{K_{D,\mathrm{TF}}}{K^{\rm ns}_{D,\mathrm{TF}}} \qquad \frac{k_{\rm b}}{k_{\rm f}} = [D]_{\rm tot} \cdot \frac{K_{D,\mathrm{RNAp}}}{K^{\rm ns}_{D,\mathrm{RNAp}}} \tag{4}$$

The human genome has about 3×10^9 bp. In a diploid cell, there are therefore about $6 \times 10^9 \approx 10^{-14}$ moles of base pairs in a volume of about $500\,\mu\mathrm{m}^3 = 5 \times 10^{-13}$ L. This gives a concentration of $[\mathrm{D}]_{\rm tot} = 0.02\,\mathrm{M} = 20\,\mathrm{mM}$. Protein-DNA dissociation constants have been found to range widely, with reported values for transcription factor-DNA binding ranging from micromolar to picomolar (9, 10) or even stronger (11), with nanomolar values being common. We have been using dissociation constants of 1 nM for specific binding of TF or RNAp. The resulting values of the dissociation rates are

$$k_{\rm o} = (0.05\,\mathrm{nM}^{-1}\mathrm{s}^{-1}) \cdot (20\,\mathrm{mM}) \cdot \frac{1\,\mathrm{nM}}{1\,\mathrm{mM}} = 1.0\,\mathrm{s}^{-1} \tag{5}$$

$$k_{\rm b} = (0.03\,\mathrm{nM}^{-1}\mathrm{s}^{-1}) \cdot (20\,\mathrm{mM}) \cdot \frac{1\,\mathrm{nM}}{1\,\mathrm{mM}} = 0.6\,\mathrm{s}^{-1} \tag{6}$$

The inverse of the rate k_m represents the time taken by the polymerase (once already bound to the promoter) to initiate transcription, as well as to produce the pre-mRNA transcript. An average initiation time of one minute (12) gives

$$k_{m,0} = 0.02\,\mathrm{s}^{-1}$$

In the model, the step in which nuclear mRNA becomes cytoplasmic mRNA (with rate γ) includes nucleocytoplasmic diffusion to a nuclear pore in addition to directed transport across the nuclear pore. The transport and export of mRNAs has been studied at the single-molecule level in Drosophila by

Mor et al. (13) who report that nucleocytoplasmic diffusion to a nuclear pore complex (NPC) occurs on a timescale of 5–40 minutes, while directed transport across the NPC occurs much more rapidly. Assuming a mean time scale of 20 minutes for an mRNA to exit the nucleus from the site of splicing, we have

$$\gamma_0 = 8 \times 10^{-4}\,\mathrm{s}^{-1}$$

The rate of degradation of mRNA in the cytoplasm varies from one transcript to another(14, 15); we use a typical time scale of about one hour to arrive at

$$\nu_0 = 3 \times 10^{-4}\,\mathrm{s}^{-1}$$

We now must estimate the total concentration (bound as well as free) of promoters, RNA polymerases, and transcription factors. Here a question arises as to how to interpret our model: are we describing a single gene and its specific transcription factors, as did Morelli et al.(16), or rather describing in a coarse-grained way all of the genes at once? In the former case the concentration of promoters in a diploid cell is $2/V$ where V is the volume of the nucleus, while in the latter case we must take into account the total number of active genes. We choose to include all of the active genes at once, to include the possibility that changes in binding affinities (for example, as the level of crowding is changes) for such a significant number of genes might affect the concentration of free RNAp or TF. Experiments in HeLa cells (17) suggest a number of RNAp molecules on the order of 10^4, with numbers of general transcription factors (such as TBP) of the same order of magnitude. Likewise, in a genome with tens of thousands of genes the number of binding sites O is of the same magnitude. Given that the nuclei of these cells have volumes (4, 5) on the order of $V_{\mathrm{nuc}} = 500\,\mu\mathrm{m}^3 = 5 \times 10^{-13}\,\mathrm{L}$ we have

$$[\mathrm{TF}]_{\mathrm{tot}} \approx [\mathrm{RNAp}]_{\mathrm{tot}} \approx [\mathrm{O}]_{\mathrm{tot}} \approx \frac{10^4}{V_{\mathrm{nuc}}} \approx 30\,\mathrm{nM}$$

These are clearly rough estimates, and for many reasons we should consider a wide range of possible concentrations. The distributions of molecules in the nucleus involved in transcription are non-uniform, and we might choose to interpret our concentrations as the local values at the site of transcription (for example, in transcription factories), since the local concentrations are the only relevant ones for the binding reactions. Furthermore, many promoter binding sites will be bound by nucleosomes and inaccessible to DNA-binding proteins, so that the concentration of "active" genes may be reduced compared to the total number of genes.

2 Diffusion Coefficients: Brownian Dynamics simulations

To find the crowding dependence of the diffusion coefficients of TF and RNAp in our model, we performed Brownian Dynamics (BD) simulations of spherical tracer particles of various radii diffusing among spherical crowders of radius 3 nm. These simulations were carried out using the GROMACS package (18). The purely repulsive interaction potential between two spherical particles (either crowders or tracers) of radii r_1 and r_2 was

$$U(r) = 4\epsilon \left(\frac{\sigma}{x + \sigma - r_1 - r_2} \right)^{12}, \tag{7}$$

with $\epsilon = 1\,\mathrm{kJ/mol}$ and $\sigma = 1\,\mathrm{nm}$. According to the Stokes formula, the friction coefficient γ of a sphere is proportional to its radius. In our simulations we have used drag coefficients of $\gamma = r \cdot 30\,\mathrm{amu/ps} = r \cdot 30\,\mathrm{kJ \cdot ps/mol \cdot nm^2}$ where r is the radius of a molecule (crowder or tracer). Our simulations were performed at a temperature of 310 K, although the results of the simulations (diffusion coefficients normalized by their crowder-free values) should be nearly independent of temperature since our interaction potentials are nearly hard-sphere potentials.

For each tracer particle radius we performed simulations at many different levels of crowding by including different numbers of crowders within a $(63\ \mathrm{nm})^3$ simulation box. The number of 3 nm radius crowders in the box varied from 30 to 1140 in steps of 30, corresponding to volume fractions up to about $\phi = 0.5$.

From each simulation trajectory the diffusion coefficient of the tracer particle was determined as one sixth of the average slope of the particle's mean-square displacement over the time interval from $t = 5\,\mathrm{ns}$ to $t = 20\,\mathrm{ns}$. The diffusion coefficients were then normalized to their values in the absence of crowding. The resulting normalized diffusion coefficients are shown in Fig. 1. These sets of simulations were performed for tracer particles of radii 2,4,5, and 6 nm; for tracer particle radius of 3 nm we used simulations with crowders only. The normalized diffusion coefficients were well fit by a cubic polynomial in ϕ, namely

$$\frac{D(\phi, r)}{D(0, r)} \equiv f(\phi, r) = 1 + \alpha \left(\frac{r}{r_{\mathrm{crowd}}} \right) \phi + \beta \left(\frac{r}{r_{\mathrm{crowd}}} \right) \phi^2 + \gamma \left(\frac{r}{r_{\mathrm{crowd}}} \right) \phi^3, \tag{8}$$

here α, β, and γ are fitting parameters, depending only on the ratio of the tracer particle radius to the crowder radius, which are given in Table 1. For

r/r_{crowd}	α	β	γ
2/3	-1.41	0.40	-2.23
3/3	-1.95	1.10	-1.91
4/3	-2.83	3.87	-4.11
5/3	-3.57	6.46	-6.45
6/3	-4.39	9.69	-9.76

Table 1: Coefficients in Eqn. 8 for a cubic fit to $f(\phi)$.

the model discussed in the article, we need normalized diffusion coefficients for tracer particles of radius 4 and 5.4 nm, representing the transcription factor and the RNA polymerase, respectively. For the transcription factor, we use Eqn. 8 above with the fitting parameters for $r = 4$ nm. For the RNAp, we did not have simulations of tracers with radius precisely equal to 5.4 nm, so for the polymerase's diffusion coefficient we have used Eqn. 8 with fitting parameters obtained by interpolating the data of Table 1: namely $\alpha = -3.89$, $\beta = 7.72$, and $\gamma = -7.72$.

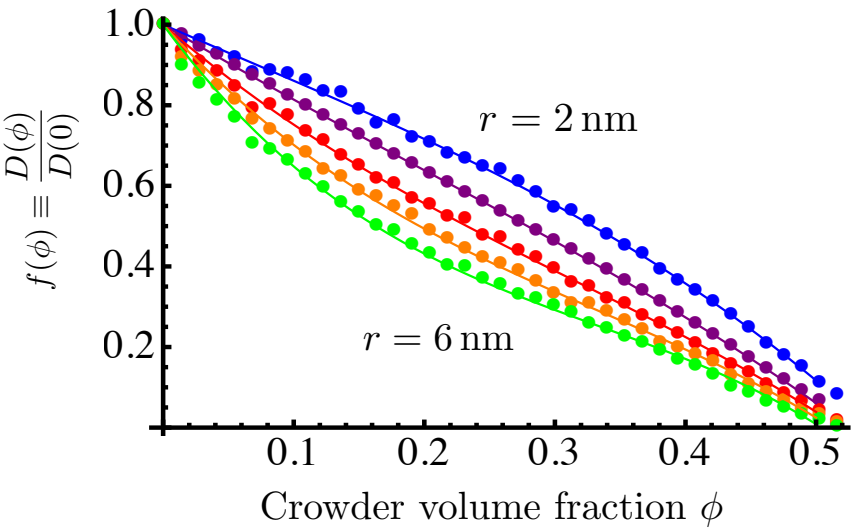

Figure 1: The factor f by which the diffusion coefficient of a tracer molecule is decreased by the presence of a volume fraction ϕ of crowders (radius 3 nm). This is shown for various radii of tracer molecules: 2, 3, 4, 5, and 6 nm (top to bottom). Brownian Dynamics simulations are shown with dots; the curves are polynomial fits given by Eq. 8 with parameters given in Table 1.

3 Crowding-mediated interactions: Monte Carlo simulations

To calculate the crowding-induced contribution $\Delta F_{\rm crowd}(\phi)$ to the binding free energies, as well as the crowding-induced free energy barrier to association $\Delta F_{\rm barrier}(\phi)$, we have performed Monte Carlo simulations, which we discuss now in the context of TF binding to DNA; the case of RNAp binding to DNA is similar. In each simulation, the cubic simulation box of size $(50\ {\rm nm})^3$ contains the TF (a sphere of radius 4 nm) as well as the DNA (a row of 50 overlapping spheres of radius 1 nm, spaced 1 nm apart, approximating a rod of diameter 2 nm) and some number $N_{\rm crowd}$ of crowders. The crowders interact with each other, and with the spheres making up the TF and DNA, as impenetrable hard spheres. The Monte Carlo moves are random small translations of randomly selected crowders. These moves are rejected if they cause any overlap between the crowders or between crowders and the TF or DNA, and accepted otherwise. Every 10 MC moves, a test move is considered which increases the distance between the TF and DNA by 0.1 nm (this distance is the reaction coordinate). Likewise, a test move is also considered which decreases this distance by 0.1 nm. Like the MC moves, the test moves are accepted or rejected based on whether they lead to overlaps between crowders and TF or DNA. Over the course of millions of MC moves, this gives a numerical estimate of the probability $p_{\rm forward}$ of accepting a move that increases the reaction coordinate, as well as the probability $p_{\rm backward}$ of accepting the reverse move. The free energy change in increasing the TF-DNA distance by $\Delta x = 0.1$ nm is then given by (19)

$$\beta \Delta F_{\rm crowd}(x \to x + \Delta x) = \ln \left[\frac{p_{\rm backward}}{p_{\rm forward}} \right], \tag{9}$$

where $\beta = 1/k_B T$. From the free energy changes for each small step of size Δx, we map out the potential of mean force (PMF) between the TF and the DNA (see Fig. 1c of the article). As shown in this figure, the PMF reaches a plateau value which is the free energy required to separate the TF from the DNA against the depletion force caused by the crowders, or equivalently minus the crowder contribution to the free energy of binding. The difference between the maximum of the PMF and the plateau value gives the crowder-mediated free energy barrier $\Delta F_{\rm barrier}$ to association. These sets of simulations were performed for numbers of crowders between 20 and 440 in steps of 20, corresponding to nuclear crowder volume fractions from $\phi =$ 0.018 to 0.4. The resulting free energies and free energy barriers are plotted

in Fig. 2 and Fig. 3 respectively. Likewise, the crowding-induced free energy difference for pulling RNAp away from DNA is shown in Fig. 4 and the corresponding free energy barriers in Fig. 5. Finally, the change in excluded volume as the RNAp slides into contact with the TF along the DNA (forming the complex C_{II}) entails a crowding-induced free energy change, which we have also calculated. This is shown in Fig. 6, with the corresponding free energy barrier plotted in Fig. 7. The free energies determined from the Monte Carlo simulations were well fit by the following expressions.

$$\begin{aligned}
-\beta\Delta F_{\mathrm{crowd,TF}}(\phi) &= 3.2\,\phi + 2.0\,\phi^2 \qquad -\beta\Delta F_{\mathrm{barrier,TF}}(\phi) = 2.5\,\phi^2 \\
-\beta\Delta F_{\mathrm{crowd,RNAp}}(\phi) &= 3.7\,\phi + 2.7\,\phi^2 \qquad -\beta\Delta F_{\mathrm{barrier,RNAp}}(\phi) = 3.1\,\phi^2 \\
-\beta\Delta F^{\mathrm{slide}}_{\mathrm{crowd,RNAp\text{-}TF}}(\phi) &= 2.6\,\phi + 4.6\,\phi^2 \qquad -\beta\Delta F^{\mathrm{slide}}_{\mathrm{barrier,RNAp\text{-}TF}}(\phi) = 0.1\,\phi^2 + 9.2\,\phi^3
\end{aligned}$$

The Monte Carlo simulations were implemented using a C program whose code is available from the authors upon request.

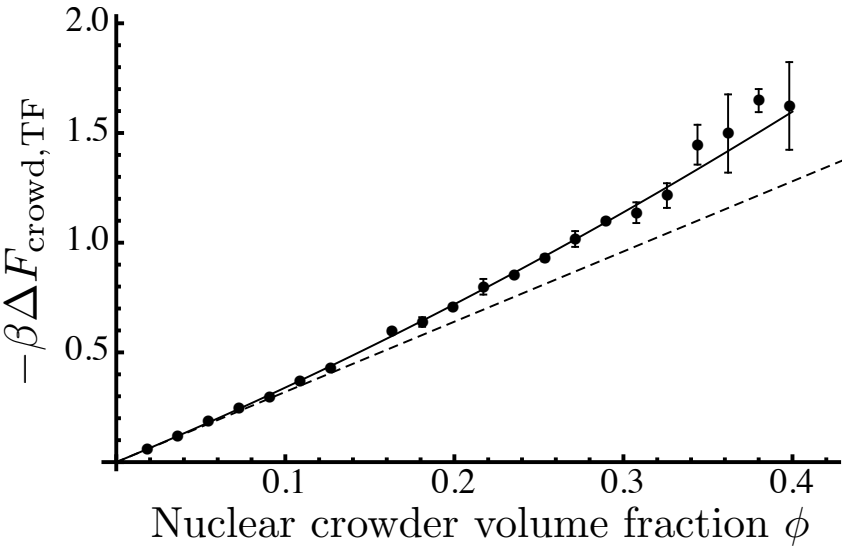

Figure 2: Crowding induced free energy change associated with TF-DNA binding. Symbols show the results of Monte Carlo simulations with error bars given by the standard error of four independent simulations. The solid line shows the polynomial fit $-\beta\Delta F_{\mathrm{crowd,TF}}(\phi) = 3.2\,\phi + 2.0\,\phi^2$ used in computing the results in the paper. The dashed line shows the linear approximation $-\beta\Delta F_{\mathrm{crowd,TF}}(\phi) = 3.2\,\phi$ that can be obtained by exact integration of excluded volume overlaps.

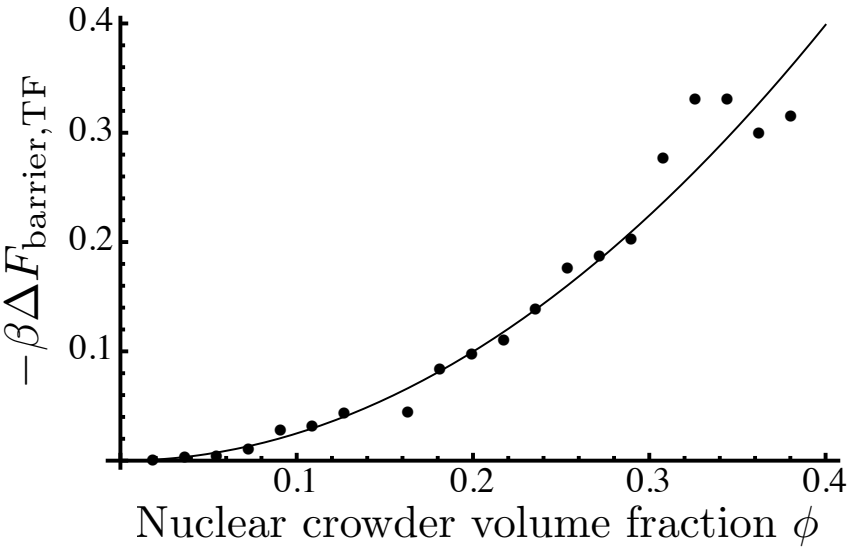

Figure 3: Crowding induced free energy barrier associated with TF-DNA binding. Symbols show the results of Monte Carlo simulations.The solid line shows the polynomial fit $-\beta\Delta F_{\mathrm{barrier,TF}}(\phi) = 2.5\,\phi^2$ used in computing the results in the paper.

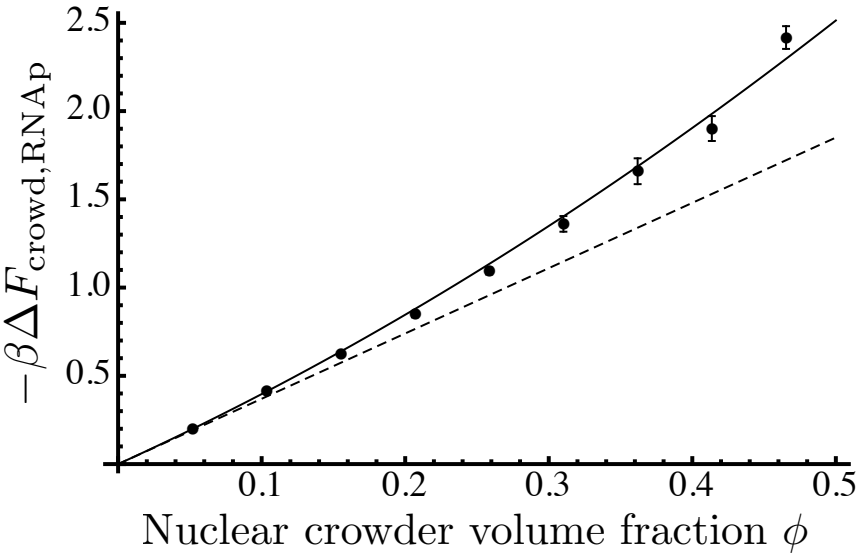

Figure 4: Crowding induced free energy change associated with RNAp-DNA binding. Symbols show the results of Monte Carlo simulations with error bars given by the standard error of ten independent simulations. The solid line shows the polynomial fit $-\beta\Delta F_{\mathrm{crowd,RNAp}}(\phi) = 3.7\,\phi + 2.7\,\phi^2$ used in computing the results in the paper. The dashed line shows the linear approximation $-\beta\Delta F_{\mathrm{crowd,RNAp}}(\phi) = 3.7\,\phi$ that can be obtained by exact integration of excluded volume overlaps.

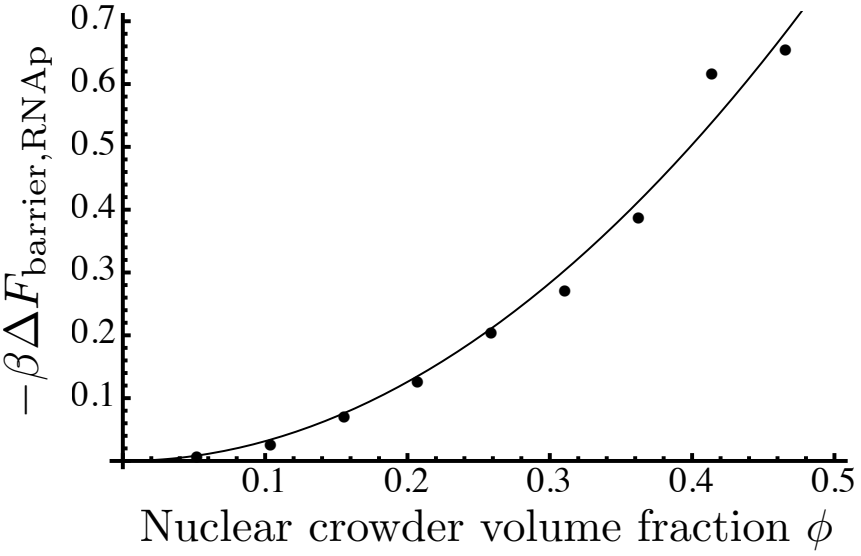

Figure 5: Crowding induced free energy barrier associated with RNAp-DNA binding. Symbols show the results of Monte Carlo simulations.The solid line shows the polynomial fit $-\beta\Delta F_{\text{barrier,TF}}(\phi) = 3.1\,\phi^2$ used in computing the results in the paper.

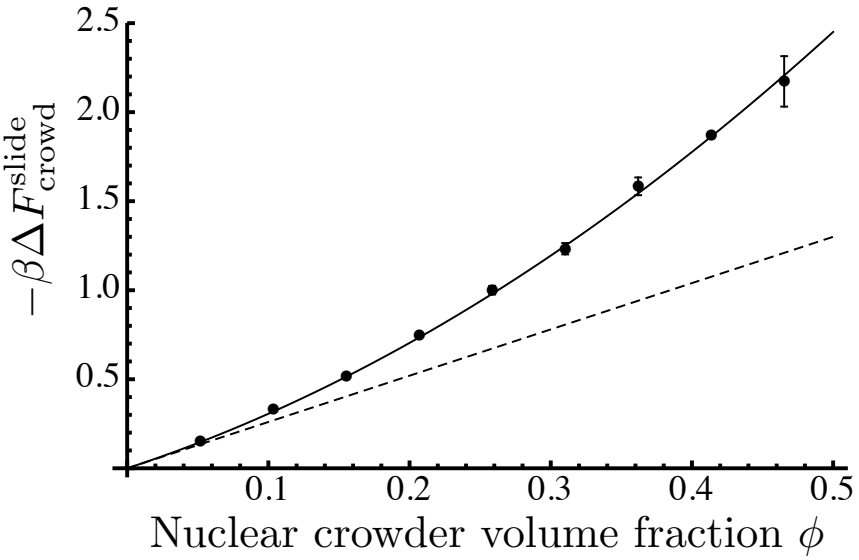

Figure 6: Crowding induced free energy change associated with RNAp "sliding" toward TF along DNA, forming complex C_{II}. Symbols show the results of Monte Carlo simulations with error bars given by the standard error of ten independent simulations. The solid line shows the polynomial fit $-\beta\Delta F^{\rm slide}_{\rm crowd,RNAp\text{-}TF}(\phi) = 2.6\,\phi + 4.6\,\phi^2$ used in computing the results in the paper. The dashed line shows the linear approximation $-\beta\Delta F^{\rm slide}_{\rm crowd,RNAp\text{-}TF}(\phi) = 2.6\,\phi$ that can be obtained by exact integration of excluded volume overlaps.

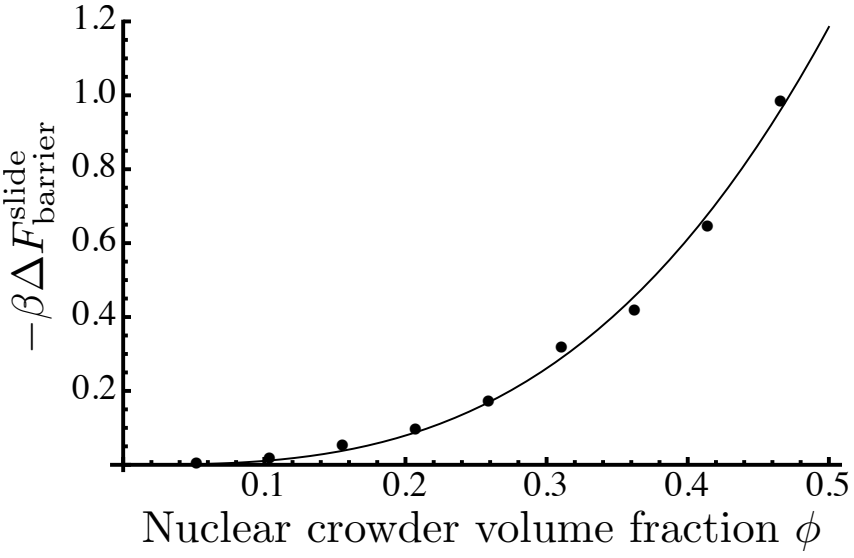

Figure 7: Crowding induced free energy barrier associated with RNAp "sliding" toward TF along DNA, forming complex C_{II}. Symbols show the results of Monte Carlo simulations. The solid line shows the polynomial fit $-\beta\Delta F^{\rm slide}_{\rm barrier,RNAp\text{-}TF}(\phi) = 0.1\,\phi^2 + 9.2\,\phi^3$ used in computing the results in the paper.

4 Effects of Crowder Polydispersity

In order to ensure that our results are not dependent on the strict monodispersity of crowders in the model, we have performed some Monte Carlo simulations to calculate the crowding induced free energy change upon RNAp binding to DNA, using a small level of crowder polydispersity. Specifically, we used crowders with a distribution of three sizes: small (2.7 nm), medium (3.0 nm), and large (3.3 nm). Half of the crowders were of medium size and 25% were small and large. Figure 8 shows that this poly-dispersity does not significantly affect the results.

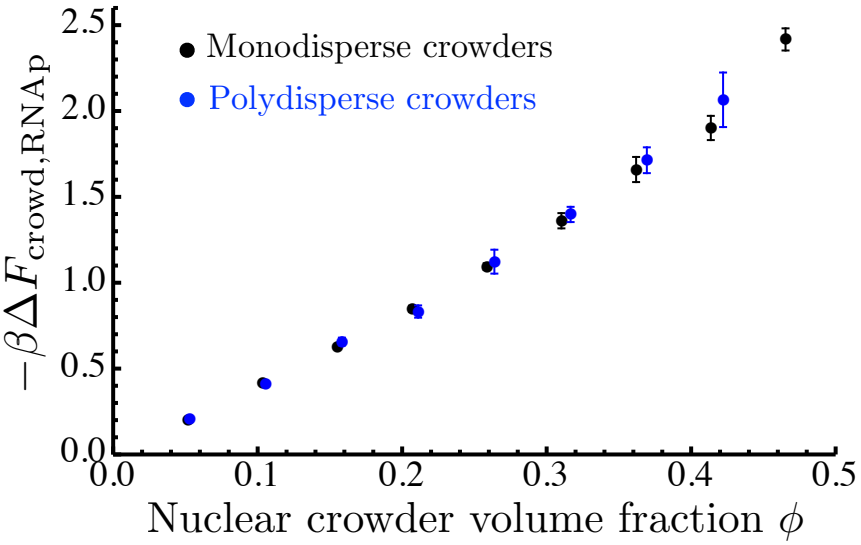

Figure 8: Effects of crowder polydispersity on the crowding induced free energy change upon RNAp binding to DNA.

References

[1] Berg, O., 1978. On Diffusion-Controlled Dissociation. *Chemical Physics* 31:47–57.

[2] Berg, O., R. Winter, and P. von Hippel, 1981. Diffusion-Driven Mechanisms of Protein Translocation on Nucleic Acids. 1. Models and Theory. *Biochemistry* 20:6929–6948.

[3] Li, G.-W., O. Berg, and J. Elf, 2009. Effects of macromolecular crowding and DNA looping on gene regulation kinetics. *Nat Phys* 5:294–297.

[4] Maul, G. G., and L. Deaven, 1977. Quantitative Determination of Nuclear Pore Complexes in Cycling Cells with Differing DNA Content. *J Cell Biol* 73:748–760.

[5] Monier, K., J. G. Armas, S. Etteldorf, P. Ghazal, and K. Sullivan, 2000. Annexation of the inter chromosomal space during viral infection. *Nat Cell Biol* 2:661–665.

[6] Elf, J., G. Li, and X. Xie, 2007. Probing Transcription Factor Dynamics at the Single-Molecule Level in a Living Cell. *Science* 316:1191–1194.

[7] Blainey, P., G. Luo, S. Kou, W. F. Mangel, G. L. Verdine, B. Bagchi, and X. Xie, 2009. Nonspecifically bound proteins spin while diffusing along DNA. *Nat. Struct. Mol. Biol.* 16:1224–1230.

[8] Bagchi, B., P. Blainey, and X. Xie, 2008. Diffusion Constant of a Nonspecifically Bound Protein Undergoing Curvilinear Motion along DNA. *J. Phys. Chem. B* 112:6282–6284.

[9] Geertz, M., D. Shore, and S. Maerkl, 2012. Massively parallel measurements of molecular interaction kinetics on a microfluidic platform. *Proc Natl Acad Sci U S A* 109:16540–16545.

[10] Nalefski, E., E. Nebelitski, J. A. Lloyd, and S. Gullans, 2006. Single-Molecule Detection of Transcription Factor Binding to DNA in Real Time: Specificity, Equilibrium, and Kinetic Parameters. *Biochemistry* 45:13794–13806.

[11] Zabel, U., R. Schreck, and P. Baeuerle, 1991. DNA Binding of Purified Transcription Factor NF-κB. *J Biol Chem* 266:252–260.

[12] Darzacq, X., Y. Shav-Tal, V. de Turris, Y. Brody, S. M. Shenoy, R. D. Phair, and R. H. Singer, 2007. In vivo dynamics of RNA polymerase II transcription. *Nat Struct Mol Biol* 14:796–806.

[13] Mor, A., S. Suliman, R. Ben-Yishay, S. Yunger, Y. Brody, and Y. Shav-Tal, 2010. Dynamics of single mRNP nucleocytoplasmic transport and export through the nuclear pore in living cells. *Nat Cell Biol* 12:543–554.

[14] Yang, E., E. van Nimwegen, M. Zavolan, N. Rajewsky, M. Schroeder, M. Magnasco, and J. E. D. Jr., 2003. Decay Rates of Human mRNAs: Correlation With Functional Characteristics and Sequence Attributes. *Genome Res* 13:1863–1872.

[15] Schwanhäusser, B., D. Busse, N. Li, G. Dittmar, J. Schuchhardt, J. Wolf, W. Chen, and M. Selbach, 2011. Global quantification of mammalian gene expression control. *Nature* 473:337–342.

[16] Morelli, M., R. Allen, and P. ten Wolde, 2011. Effects of Macromolecular Crowding on Genetic Networks. *Biophys J* 101:2882–2891.

[17] Kimura, H., Y. Tao, R. Roeder, and P. Cook, 1999. Quantitation of RNA Polymerase II and Its Transcription Factors in an HeLa Cell: Little Soluble Holoenzyme but Significant Amounts of Polymerases Attached to the Nuclear Substructure. *Mol Cell Biol* 19:5383–5392.

[18] Hess, B., C. Kutzner, D. van der Spoel, and E. Lindahl, 2008. GROMACS 4: Algorithms for Highly Efficient, Load-Balanced, and Scalable Molecular Simulation. *J Chem Theory Comput* 4:435–447.

[19] Bennett, C. H., 1976. Efficient Estimation of Free Energy Differences from Monte Carlo Data. *J Comput Phys* 22:245–268.